1-1-1987

Doppler-Free Polarization Spectroscopy Of The B1-Pi-U-X1-Sigma-G+ Band System Of K-2

J. Heinze

U. Schühle

F. Engelke

C. D. Caldwell
University of Central Florida

Doppler-free polarization spectroscopy of the $B\,^1\Pi_u - X\,^1\Sigma^+_g$ band system of K_2

Cite as: J. Chem. Phys. **87**, 45 (1987); https://doi.org/10.1063/1.453591
Submitted: 23 December 1986 . Accepted: 06 March 1987 . Published Online: 31 August 1998

J. Heinze, U. Schühle, F. Engelke, and C. D. Caldwell

Doppler-free polarization spectroscopy of the $B\,^1\Pi_u$–$X\,^1\Sigma_g^+$ band system of K_2

J. Heinze, U. Schühle, and F. Engelke
Fakultät für Physik, Universität Bielefeld, 4800 Bielefeld, West Germany

C. D. Caldwell
Department of Physics, University of Central Florida, Orlando, Florida 32816

(Received 23 December 1986; accepted 6 March 1987)

The $B\,^1\Pi_u$–$X\,^1\Sigma_g^+$ band system of the K_2 molecule is investigated by Doppler-free polarization spectroscopy in a heat pipe oven. The transitions are measured in the region of 615 to 660 nm including vibrational levels up to $v'' = 17$ in the X state and all vibrational levels of the B state up to the dissociation limit. A Fabry–Perot interferometer is calibrated using metastable neon and K_2 secondary wavelength standards to provide absolute accuracy in the frequency determination of less than 20 MHz. The comprehensive study of the band system is completed by LIF measurements to determine vibrational levels of the ground state up to $v'' = 62$. A detailed analysis has been completed and the coefficients are given in a Dunham expansion that accurately represents the frequencies of lines with specified vibrational and rotational quantum numbers. The B and X potential curves and the Franck–Condon factors for the transitions between B and X states are determined. The dissociation energies have been found to be 4447 ± 15 cm^{-1} for the X state and 2113 ± 15 cm^{-1} for the B state. The height of the potential barrier of the B state above the $4\,^2P_{3/2} + 4\,^2S_{1/2}$ atomic levels is 295 ± 17 cm^{-1} at an internuclear distance of 8.1 ± 0.1 Å.

I. INTRODUCTION

High resolution laser spectroscopy has been responsible for a considerable increase in the detailed understanding of molecular structure during the past 20 years. Many techniques for Doppler-free spectroscopy are now available and a wide variety of molecular transitions in the visible have been studied with the help of tunable lasers.

The combination of a single-mode dye laser with either a molecular beam or a polarization spectrometer makes possible spectroscopic determinations of molecular wavelengths at a very high resolution. These techniques have proven to be fruitful for analysis of the spectra of the alkali dimers.[1–3] At the high resolution obtainable with these schemes, <30 MHz, calibration of absolute frequencies becomes more difficult. For this to be properly done, it is necessary to utilize optical interferometry in conjunction with the measurements.

While wavelength measurements utilizing a crossed laser-atomic beam are ultimately slightly more accurate than those employing polarization spectroscopy in a cell,[4] it is difficult to acquire data by this method throughout the entire electronic transition to allow description of the system via a set of molecular vibrational and rotational constants. The cooling resulting from expansion in a molecular beam reduces the necessary population in the higher-lying rotational and vibrational levels. The technique of polarization spectroscopy[5] thus provides the necessary continuation of the spectral analysis to include these levels.

Two years ago we reported[2] the determination of six absolute transition frequencies in the (6–0) band of the $B\,^1\Pi_u$–$X\,^1\Sigma_g^+$ band system of the $^{39}K_2$ dimer to within an accuracy of three parts in 10^9. Earlier, Amin[6] had reported the measurements of three neon transitions to within an accuracy of one part in 10^9. These three neon transitions, together with the six K_2 transitions, provide an excellent secondary wavelength standard for calibration of an interferometer where we adopted the definition of the meter referred to in Ref. 2. Using these results, we have extended our high-resolution work on the K_2 dimer to include measurements throughout the upper state potential curve and in the ground-state curve up to $v'' = 17$ using polarization spectroscopy. Absolute wavelength determinations are carried out in an interferometer calibrated with the secondary standard.[2] We use the results to determine a set of molecular constants to describe this band system, at least in that portion of the spectrum which we have measured.

Molecular constants for the X state and the B state of K_2 have been known since the early work of Loomis and Nusbaum[7] and Loomis.[8] The same electronic transition was also the first utilized for the application of laser induced fluorescence to molecular spectroscopy by Tango, Link, and Zare.[9] They took advantage of a fortuitous overlap of the He–Ne laser with several of the molecular transitions. From their analysis they determined constants for the $^1\Sigma_g^+$ ground state. Allegrini *et al.*,[10] extended the LIF analysis using a Kr^+ laser and were able to deduce constants for the B state as well. Engelke *et al.*,[1] using crossed-beam two-photon ionization techniques, were able to improve the accuracy of the measurements and devise new, improved constants for both states. Their work led to the conclusion that the rotational assignments of Refs. 9 and 10 were incorrect. However, the data base in this experiment was too small to allow determination of constants appropriate for higher-lying rotational and vibrational levels. More recently, excitation with a gold-vapor laser[11] and with a Kr^+ laser and a dye laser[12] has led to

 0021-9606/87/130045-09$02.10

a rederivation of the ground-state constants. In the latter work, Ross and co-workers extended the observed vibrational levels of the X state up to $v'' = 55$. The results obtained provide accurate determination of the ground-state potential curve up to $v'' = 50$.[12]

We present here assignments of over 2500 rovibrational transitions within the K_2 $B\,^1\Pi_u$–$X\,^1\Sigma_g^+$ band and report for the first time a set of molecular constants for the $B\,^1\Pi_u$ state valid up to $v' = 40$ (96% of the bound and quasibound part of this state) and for the $X\,^1\Sigma_g^+$ state valid up to $v'' = 62$ (94% of the ground state).

II. EXPERIMENTAL

The polarization spectrometer used in these measurements along with the optical layout is sketched in Fig. 1. The K_2 is produced in a heat pipe which is heated to a temperature of 530 K. Helium is used as a buffer gas, and operation at this temperature produces a pressure of 0.1 mbar. An Ar^+ pumped ring dye laser externally stabilized to a width of 1 MHz serves as the excitation source. For the ultraprecise measurements the beam from the dye laser is split into two, so that one portion serves as pump and the second as probe. This way both pump and probe beams have the same frequency. For the measurement of P and R transitions, the pump beam is circularly polarized; for the measurements of Q lines, the pump beam is linearly polarized. The probe beam is analyzed by a combination of crossed linear polarizers with an extinction coefficient lower than 10^{-8}. Typical signal-to-noise ratios obtainable with this arrangement are 10 : 1 to 1000 : 1. Therefore, it is unnecessary to employ phase sensitive detection techniques.

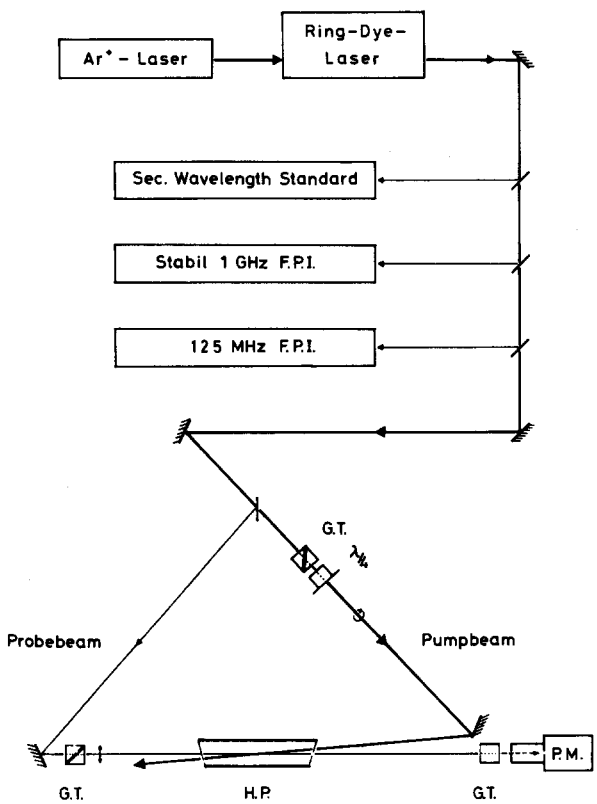

FIG. 1. Experimental arrangement of the polarization spectrometer together with the wavelength calibration system used to determine the absolute frequencies of the K_2 transitions. HP: heat-pipe oven; GT: Glan-Thomson prism; PM: photomultiplier.

The interferometer in which wavelength comparisons were made consists of two plane-parallel mirrors optically contacted to a 15 cm long piece of zerodur. The mirrors are broad-band high-reflection coated with dielectric materials with a central wavelength of 640 nm and a bandwidth of 200 nm (FWHM). A typical finesse of 70 during a scan is considered an appropriate operating point.

The measurement of absolute wavelengths via optical interferometry is difficult when the mirrors are dielectric coated. This comes about because the phase shift at the mirrors is wavelength dependent. Rather than being equal to π, as is the case with metallic mirrors, the shift can deviate from π. However, Lichten[13,14] has shown that it is possible to calculate the phase shift within the bandwidth of the mirror coating if the reflectivity is known throughout the entire bandwidth. From reflection curves supplied by the manufacturer (B. Halle, Nachfolg., Berlin) and a measured transmission spectrum of the mirrors we have calculated the phase shift as a function of wavelength using Lichten's method[14]; it consists of fitting the transmission spectrum with an equivalent quarterwave stack numerically. Within about 2% of the phase shift, at most a few thousandths of an order, this method is most usable for measuring absolute wavelength.

The free spectral range of the interferometer was determined by calibration with the three neon secondary standard wavelengths at 6266, 6334, and 6533 Å.[6] For this purpose a metastable neon beam source was constructed.[15] Measurements were carried out by crossing the well-collimated neon beam with the dye laser and determining the proper transition frequency through reduction in neon beam intensity as the metastable atoms are excited. By counting fringes from one wavelength to another, the integral order number could be determined exactly.

The primary difficulty associated with the determination of the free spectral range of the etalon was the drift associated with temperature changes in the environment. For this particular device, this drift produced a change in the order number of 0.01/h. In order to account for this drift, comparison with the K_2 (6–0) $R(29)^2$ transition was carried out repeatedly during the course of a measurement. The final free spectral range is 1001.7637 $\pm$ 0.0002 MHz, whereby the error is primarily determined by the long-term temperature drift.

For a typical measurement the following procedure was used. After calibration with the K_2 transition, the dye laser was tuned to the wavelength region of interest. The laser was then scanned through a typical frequency range of 200 GHz in steps of 30 GHz. First, circularly polarized light was used to select the P and R transitions. Then linearly polarized light in the same frequency range was used to isolate the Q transitions. Frequency monitoring was always possible as P and R transitions appear with linearly polarized pump radi-

ation as well, only with reduced intensity. The signal from the probe beam was recorded in a four-channel chart recorder along with the marks from the etalons. The principal error in the frequency measurement arises from a combination of uncertainties in this scheme. The laser scan, which ideally should be linear, is not. The nonlinearity is partially corrected for by the 125 MHz etalon marks. However, this device itself exhibits drifts in free spectral range. In addition, the final separation between laser frequency, measuring etalon, and frequency marker has to be read from the chart paper. Thus, nonlinearities in the chart speed also contribute to errors in the final measurement. By repeating measurements at several different wavelengths, the total error associated with all these shifts was estimated to be $\pm$ 10 MHz.

In addition to the wavelengths to which particular attention was devoted, measurements were also carried out on other parts of the bands, see Fig. 2. In these regions, the combination of errors listed above gave rise to larger deviations, generally on the order of 20 MHz. The primary causes of this were that faster scan speeds were used, and etalon drift corrections were not as frequently determined.

The problem associated with the use of a heatpipe for spectroscopic measurements at this level of accuracy is the pressure shift which is produced on the lines. We have made an extensive study of this shift for different buffer gases.[16] The largest shift is produced by the potassium atoms themselves and amounts to 10 MHz/mbar. At our experimental conditions, 0.1 mbar, this produces a frequency shift of $\leqslant 1$ MHz. The frequencies which we include in our fit have been corrected for this effect. The absolute frequencies of lines, free of distortion, are thus determined to better than 0.0005 cm^{-1}.

In order to extend measurements to higher vibrational levels of the ground state we also made laser induced fluorescence studies in a separate heat pipe. For this experiment the dye laser is locked to the polarization signal of suitable transitions to high vibrational levels in the B state ($v' = 34$, $J' = 60$ and $v' = 40, J' = 30$). Part of the laser light is used to excite these transitions in a second heat pipe. Fluorescence is then dispersed by a 3/4 m spectrograph (SPEX 1702) and detected by a photomultiplier (RCA 31034). The width of the measured lines is about 0.3 cm^{-1}. The spectrograph is calibrated by a neon filled hollow cathode discharge lamp and absolute frequencies of lines, free of distortion are determined to better than 0.5 cm^{-1}.

III. RESULTS

Wavelength measurements using polarization spectroscopy were carried out in the region 615 to 660 nm. These included transitions up to $v'' = 17$ in the ground state and $v' = 43$ in the B state.[17] In addition to these, we also made determinations of some transitions up to $v''_{max} = 62$ using lower resolution laser induced fluorescence. In what follows we will distinguish two energy regimes for the very high resolution data: (1) A lower one for $v''_{max} = 9$ and $v'_{max} = 21$; and (2) a middle region for $v''_{max} = 17$ and $v'_{max} = 40$. The spread of the data set accumulated using polarization spectroscopy over the two groups is given in Fig. 2. Here the number at a particular point represents the number of lines within $\Delta J = 10$ for a given v' and v'' which will be included in the analysis. Boldface type indicates that at least one of the transitions was measured with an accuracy of 10 MHz; the remaining were measured with an accuracy of 20 MHz.

The starting point in the process of assigning quantum numbers to observed lines is the molecular beam work[1]; we extended this earlier rather detailed analysis of the TPI spectrum of the B–X system at relatively low vibrational ($v'' < 2$, $v' < 12$) and rotational ($J < 100$) quantum numbers. Reference 1 gave preliminary Dunham coefficients from which an

v'' \ J''	10			50				100					150					200
0	31	22	11	3	4	3	8	9	10	16	12	8	8	9	7	9	8	11	9
1	14	8	8	3	11	19	7	9	7	11	9	9	11	9	8	5	3	5	1
2	11	11	25	14	4	7	12	15	18	5	7	11	11	6	2	1	2	1	
3	8	9	12	10	10	8	14	13	6	15	15	8	13	4	5	2			
4	30	11	2	1	21	19	3	9	24	11	6	12	10	6	1				
5	22	27	11	2		3	9	17	6	8	13	6	9						
6	3	6	2	5	9	18	10	3	10	15	9	6	2	2					
7	4	3	15	17	8		5	14	7	5	4	2	1						
8				1	3	7	13	6	9	8	4	1	2						
9	4	4	4	21	8	1	3	10	7	4	4	3							
10			1	5	2	7	9	2	9	1	6								
11			7	18	3	3	4	8	4	9									
12	9	4	4		3	9	1	7	3										
13	6	5	7	4	4	10	4	7	4										
14	6	2	16	4	1	3	1												
15	5	3	3	5	1	3	1												
16		2	19	14	3	3													
17		2	5	1															

v'' \ J''	10			50				100					150					200
0	14	13	10	4	5			2	5	8	4			2	2	1		
1	4	3	2	3	4	1	3	4	3	5	4		2	6	1	3		2	2
2	1			2	5	3	2	5	7	6	3	5	6	6	4	2	4	2	
3	6	2	2			1	4	4	1		1	5	6	4	2	6	2	4	3
4	12	8	2	2	5	6	2	2	2	2	4	7	8	1	3	3	2	4	2
5	5	3	5	5	4	2		2	3	4	3	3	1	1	6	4	3	2	3
6	6	4	2	2	4	4	4	2	7	6	2	4	7	4	3			3	1
7	9	6	2		1	4	8	6	3	5	6	5	3	3	1				
8	3	1	10	5	5	4	3	3	4	3	3	2	2						
9	1	2	5	2	3	4	9	5	3	4	2	1	3	1					
10	4	8	15	7	4	8	4	6	5	3	2	3	4	2					
11	18	10	4	7	2	1	3	6	4	7	4	4	2						
12	9	6			4	4	3	7	6	1	2	3	4						
13	4	8	4		6	8	6	5	2	5	5	4							
14	12	13	4	5	11	6	2	2	6	7	5			4	1				
15	6	3				2	2	4	10	3	2	4	5						
16				5	5	5	8	8		2	5	5							
17			3	8	9	7	3	4	4	6	4		2						
18	5	4	9	4			2	7	8	5		2	4						
19						2	7	8	3	1	2	4							
20				6	9	8	2		2	8	5								
21	4	3	7	7	1			4	10	2		2	1						
22				1	1	2	11	8		1	6	1							
23				2	4	7	3		1	6	2		2						
24	4	3	8	8				3	7			3							
25				1	1	1	7	4		2	7								
26			1	6	6	4		1	4	6									
27		3	1	2			2	5	3	1	2								
28				2	3	6	3		2	2									
29	5	3	2	2			1	4	4										
30				2		4	2		3	3									
31	4		7	5				3	1										
32						2	2												
33	6	2	3	4	1			5	1										
34			1	1	5	5	2												
35	6	2	5	6	1														
36			1			3	1												
37	5	2	9	4															
38			2	3	2	4													
39		1	5	3															
40		2	6	6															

FIG. 2. Distribution of the data base throughout the vibrational levels. The number at each point refers to the number of transitions within $\Delta J = 10$ included in the fit. Boldface type indicates that the accuracy of the measurement for at least one of the transitions is $\pm$ 10 MHz; normal type $\pm$ 20 MHz. The number of lines included in our fit is 1630, the number of lines measured with high accuracy is 1000.

extrapolation of line frequencies to higher quantum numbers was made; an iterative process provided a basis for extending the body of data.

Dunham coefficients are calculated by fitting all the data—at that stage quantum numbers were assigned to 2500 lines—in a weighted linear least-square routine[18] to the well known expansion[19]:

$$\nu = T'(v',J') - T''(v'',J'') + \Delta T'(v',J'), \qquad (1a)$$

with

$$T(v,J) = \sum_{l,k} Y_{lk}(v+1/2)^l[J(J+1) - \Lambda^2]^k \qquad (1b)$$

and

$$\Delta T'(v',J') = \delta\left(\sum_{l,k} y_{lk}(v+1/2)^l[J(J+1) - \Lambda^2]^k\right), \qquad (1c)$$

where ν is the frequency of the line, the Y_{lk} are the Dunham coefficients, $\Delta T'(v',J')$ describes the Λ doubling of the excited $B\,^1\Pi_u$ state, i.e., $\delta = 0$ describes the lower f levels which give rise to the Q lines ($\Delta J = 0$) and $\delta = 1$ describes the upper e levels which give rise to the P and R lines ($\Delta J = \pm 1$).

During the progress of our analysis many determinations of the coefficients have been made for varying amounts of molecular lines and for different choices and numbers of Dunham coefficients. It is not our purpose to describe the different stages of our analysis in detail. Nevertheless, these steps were important in the determination of the molecular properties.

The final, best-fit values of the constants using the largest body of high resolution data are listed in Table I. Because of the high degree of correlation between the fit param-

TABLE I. Molecular constants of the $B\,^1\Pi_u$ and $X\,^1\Sigma_g^+$ states of $^{39}K_2$. All values are given in cm^{-1}. The numbers in parentheses that follow a quantity is the exponent of 10 that multiplies the quantity. The quoted error of a constant is one standard deviation. Note, to maintain the accuracy *all* digits are necessary. When fixing the higher constants to six figures we applied additional numerical effort (Refs. 21 and 22).

(l,k)	Y'_{lk}	$\sigma(\%)$	Y''_{lk}	$\sigma(\%)$
(0, 0)	15 377.1553	0.000		
(1, 0)	74.891 127	0.001	92.398 475	0.000 1
(2, 0)	− 0.327 448	0.16	0.325 719	0.01
(3, 0)	− 0.286 581(− 2)	5.5	− 0.604 270(− 3)	0.66
(4, 0)	0.268 488(− 3)	10.2	− 0.512 409(− 5)	3.4
(5, 0)	− 0.327 720(− 4)	8.8	− 0.112 526(− 6)	1.7
(6, 0)	0.240 397(− 5)	8.1		
(7, 0)	− 0.117 199(− 6)	7.5		
(8, 0)	0.373 686(− 8)	6.6		
(9, 0)	− 0.751 044(− 10)	5.9		
(10, 0)	0.862 803(− 12)	5.3		
(11, 0)	− 0.433 099(− 14)	4.7		
(0, 1)	0.048 223 297	0.001	0.056 186 982 5	0.001
(1, 1)	− 0.231 023 5(− 3)	0.04	− 0.211 061(− 3)	0.01
(2, 1)	− 0.262 568(− 5)	1.9	− 0.124 632(− 5)	0.44
(3, 1)	0.144 446(− 6)	8.6	− 0.154 718(− 7)	2.3
(4, 1)	− 0.245 943(− 7)	7.4	− 0.258 354(− 9)	4.3
(5, 1)	0.205 822(− 8)	8.2		
(6, 1)	− 0.116 092(− 9)	8.6		
(7, 1)	0.430 798(− 11)	8.6		
(8, 1)	− 0.102 695(− 12)	8.3		
(9, 1)	0.142 581(− 14)	7.5		
(10, 1)	− 0.882 548(− 17)	6.6		
(0, 2)	− 0.799 182 8(− 7)	0.06	− 0.831 454 4(− 7)	0.06
(1, 2)	− 0.890 136(− 9)	0.66	− 0.676 578(− 9)	0.31
(2, 2)	0.195 588(− 10)	7.9	− 0.729 598(− 11)	2.3
(3, 2)	− 0.568 648(− 11)	3.9		
(4, 2)	0.449 913(− 12)	4.1		
(5, 2)	− 0.219 178(− 13)	4.0		
(6, 2)	0.561 820(− 15)	3.6		
(7, 2)	− 0.636 908(− 17)	2.9		
(0, 3)	0.979 073(− 13)	2.5	0.119 927(− 12)	2.1
(1, 3)	0.256 351(− 14)	6.0	0.493 908(− 15)	9.1
(2, 3)	− 0.598 139(− 15)	3.9		
(3, 3)	0.357 419(− 16)	4.9		
(4, 3)	− 0.155 295(− 17)	2.5		
(0, 4)	− 0.472 403(− 18)	7.6	− 0.437 812(− 18)	8.4
(1, 4)	− 0.547 722(− 19)	3.2		
	Y'_{lk}			
(0, 1)	0.247 544(− 5)	1.1		
(1, 1)	− 0.145 197(− 7)	6.1		
(0, 2)	− 0.213 313(− 10)	7.7		

eters, the quoted accuracy does not represent an absolute standard deviation. Therefore, for each constant a total of at least six figures is given, as this number is required to reproduce the measured transitions.

That such a large number of constants are required to reproduce the measured frequencies arises from the broad spectral region over which the highly accurate measurements are made. The reproducibility of the transition frequencies reflects, as can be expected, the number and accuracy of the input data set as shown in Fig. 2. The transitions in group (1) can be calculated with the constants to an overall accuracy of 16 MHz. The overall deviation of the calculated from the measured frequencies in group (2) is on the order of 42 MHz. Specifically, those which were better measured are given to within 31 MHz and those less well determined to within 60 MHz, i.e., these deviations are systematic.

We note that the upper portion of the ground state is poorly described. However, without more precise data in this region, it is impossible to improve the constants to include these transitions at the same level of accuracy. Our results represent the lower-lying vibrational levels of the X state at the highest level of precision which we could achieve. At the same time we include all levels in the B state up to the region of the potential barrier. Nevertheless, comparison with our LIF data shows that the constants can be applied to calculation of high-lying vibrational levels in the ground state as long as a precision of only 15 GHz is required.

The last three constants y'_{lk} represent corrections to the energy levels caused by the Λ doubling in the B state. Our first set of constants for the B state had been fitted in such a fashion that the Q transitions are reproduced, while the Λ doubling represented a shift in energy for the P and R transitions. Thus the frequencies of the Q transitions are reproduced with the same precision as those of the P and R transitions, where most of the measurements were made.

Several bands of the isotopic molecules $^{39}K^{41}K$ and $^{41}K_2$ were also measured but were not included in the fit. A calculation of the transition frequencies using mass corrected molecular constants[19] gives results which are uniformly shifted with respect to the measured values by 79($\pm$ 3) MHz to higher frequencies for $^{39}K^{41}K$ molecules. The lines of the (0,0) bandhead of the $^{41}K_2$ molecule are shifted + 203 (10) MHz with respect to an equivalent[19] calculation. This result is in agreement with the value expected for the normal mass shift of electronic energy levels according to the Bohr model due to the change of reduced electron mass ($^{39}K^{41}K$: + 81 MHz, $^{41}K_2$: 160 MHz).

With the constants from Table I we have calculated rotationless potential curves for the two states using the Rydberg–Klein–Rees (RKR) procedure.[20] The calculated potential curves for both the B state and the X state are depicted in Fig. 3. The hatched regions (v' up to 40 and v'' up to 62) indicate that portion of the curves which should be best described based on the precision of our measurements, i.e., RKR turning points; extrapolations have been added to the dissociation limits, see Refs. 21 and 22. For the $B\ ^1\Pi_u$ state the accuracy leads to a precise determination of the curve up to the region of the potential barrier, v'_{max}. Calculation of the dissociation energy of the B state (see below) indicates that

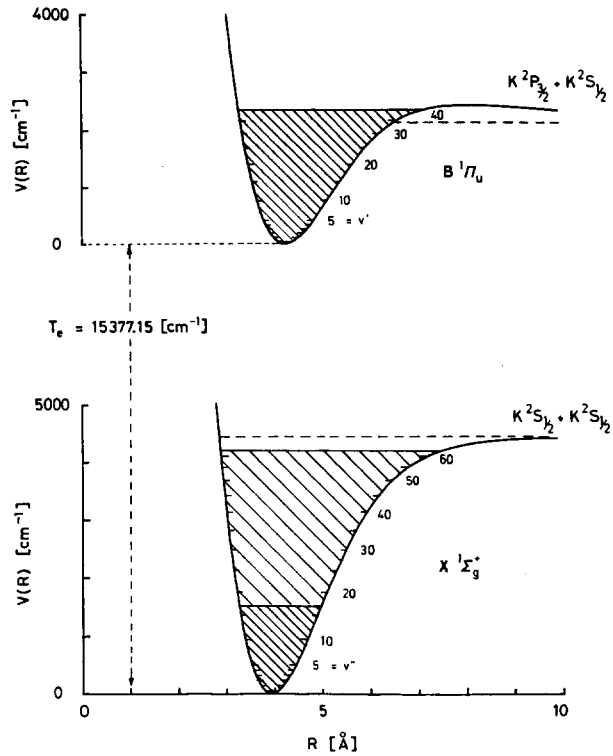

FIG. 3. Potential curves for the $B\ ^1\Pi_u$ and $X\ ^1\Sigma_g^+$ states of $^{39}K_2$ for the rotationless molecule as calculated by RKR method from the molecular constants of Table I for $v' < 40$ and $v'' < 62$ (hatched regions). Extrapolations have been added to the dissociation limits (Ref. 21).

for $v' > 34$, the states are no longer completely bound. Thus, the RKR values for this region may be expected to be inaccurate.[23] An exact description of the potential barrier will be given elsewhere[21,22]; it is not our purpose in this paper to analyze the quasibound levels in detail; let us just mention the error of the RKR values due to the coupling to the continuum is negligible for the $v' = 35$ band, but it grows up to 700 MHz for $v' = 40$.

The RKR turning points for each state are given in Tables II and III. Using these curves we than calculate Franck–Condon factors (FCF) for $J'' = 0, J' = 1$; they are listed in Table IV for $v''_{max} = 10$ and $v'_{max} = 20$. These FCF's, together with the transition diopole moment and the (thermal) population of the v,J states can be used to determine the intensities. For different choices of J we found that the FCF's are slowly varying functions of J. Table IV is useful as a guide for $J < 100$ as shown in the agreement with published intensities for the He–Ne excited fluorescence series[9] and our LIF measurements.

IV. DISCUSSION

We will discuss the dissociation energies, the centrifugal distortion constants, and the Λ-doubling constants. In addition, we will compare with previous work, i.e., recent studies of the B–X system of K_2.

In order to determine the dissociation energies we start with the ground state, because theory and experiment clearly show that the upper state has a barrier. We calculate the

ground state dissociation energy by extrapolation of the energies of the high-lying vibrational levels calculated from the set of molecular constants. We then use the method described by LeRoy and Bernstein,[24] together with the theoretical value of C_6 determined by Müller *et al.*[25] to continue the extrapolation to the dissociation limit. We obtain via this procedure the following value:

$$D_e'' = 4447 \pm 15 \text{ cm}^{-1} = 0.5514 \pm 0.0018 \text{ eV}.$$

Most of the error arises from the extrapolation of the data beyond $v'' = 62$ (94% of the dissociation energy).

The dissociation energy of the $B\,^1\Pi_u$ state D_e' can immediately be obtained using the electronic term difference T_e of 15 377.2 cm^{-1} and the energy difference of the first potassium atomic resonance transition $\nu(\text{K}\,4\,^2P_{3/2}$–$\text{K}\,4\,^2S_{1/2})$ of 13 042.9 cm^{-1}:

$$D_e'(B\,^1\Pi_u) = D_e''(X\,^1\Sigma_g^+) + \nu(4\,^2P_{3/2}\text{–}4\,^2S_{1/2}) - T_e. \tag{2}$$

Application of Eq. (2) leads to a value for the adiabatic dissociation energy of the B state

$$D_e'(B\,^1\Pi_u) = 2113 \pm 15 \text{ cm}^{-1},$$

where the error is due to the error of D_e''.

This result shows that vibrational levels in the B state with $v' > 34$ are lying above the adiabatic dissociation limit. A number of nine additional vibrational levels have now been observed in our laboratory, the last one ($v' = 43$) has an energy of 2389 cm^{-1} above the minimum of the potential and 276 cm^{-1} above the $4\,^2P_{3/2} + 4\,^2S_{1/2}$ atomic states us-

TABLE II. RKR potential of the $B\,^1\Pi_u$ state of $^{39}K_2$. The potential energy is given in cm^{-1}, the turning points are given in Å.

v'	$V(r)$	$r_{\min}$	$r_{\max}$
	0.0	4.235 99	
0	37.342	4.0899	4.3944
1	111.570	3.9898	4.5193
2	185.123	3.9241	4.6103
3	257.990	3.8725	4.6876
4	330.163	3.8291	4.7571
5	401.630	3.7913	4.8214
6	472.383	3.7576	4.8822
7	542.410	3.7271	4.9402
8	611.700	3.6991	4.9962
9	680.240	3.6732	5.0507
10	748.019	3.6492	5.1039
11	815.022	3.6266	5.1562
12	881.235	3.6054	5.2078
13	946.644	3.5854	5.2589
14	1011.231	3.5664	5.3097
15	1074.981	3.5484	5.3602
16	1137.875	3.5313	5.4107
17	1199.894	3.5149	5.4613
18	1261.019	3.4993	5.5120
19	1321.227	3.4844	5.5631
20	1380.497	3.4702	5.6146
21	1438.803	3.4565	5.6666
22	1496.120	3.4433	5.7192
23	1552.420	3.4307	5.7727
24	1607.675	3.4187	5.8270
25	1661.851	3.4071	5.8825
26	1714.916	3.3959	5.9391
27	1766.832	3.3852	5.9971
28	1817.560	3.3750	6.0567
29	1867.056	3.3651	6.1181
30	1915.274	3.3557	6.1816
31	1962.163	3.3466	6.2474
32	2007.665	3.3380	6.3158
33	2051.719	3.3297	6.3874
34	2094.256	3.3218	6.4626
35	2135.197	3.3143	6.5420

TABLE III. RKR potential of the $X\,^1\Sigma_g^+$ state of $^{39}K_2$. The potential energy is given in cm^{-1}, the turning points are given in Å.

v''	$V(r)$	$r_{\min}$	$r_{\max}$
	0.0	3.92433	
0	46.094	3.7922	4.0662
1	137.839	3.7009	4.1771
2	228.927	3.6406	4.2572
3	319.354	3.5930	4.3248
4	409.116	3.5529	4.3852
5	498.209	3.5178	4.4408
6	586.628	3.4864	4.4930
7	674.369	3.4578	4.5426
8	761.427	3.4316	4.5901
9	847.797	3.4072	4.6360
10	933.474	3.3845	4.6807
11	1018.451	3.3631	4.7242
12	1102.724	3.3429	4.7668
13	1186.286	3.3238	4.8087
14	1269.131	3.3057	4.8500
15	1351.252	3.2884	4.8908
16	1432.642	3.2718	4.9312
17	1513.294	3.2560	4.9712
20	1750.74	3.212	5.090
25	2130.94	3.149	5.287
30	2490.58	3.096	5.488
35	2828.12	3.051	5.699
40	3141.67	3.012	5.924
45	3428.96	2.978	6.173
50	3687.33	2.950	6.455
55	3913.62	2.925	6.787
60	4104.20	2.902	7.197

TABLE IV. Franck–Condon factors ($\times 10^4$), calculated from the rotationless RKR potentials of the $B\,^1\Pi_u$ and $X\,^1\Sigma_g^+$ states of the $^{39}K_2$ molecule.

v' \ v''	0	1	2	3	4	5	6	7	8	9	10
0	959	2365	2798	2106	1128	456	144	36	7	1	0
1	2099	1716	105	530	1734	1877	1193	523	171	43	8
2	2432	182	798	1229	108	426	1515	1659	1037	439	136
3	1984	211	1220	12	859	864	10	626	1538	1448	810
4	1279	1033	311	650	635	85	992	453	52	968	1552
5	694	1454	38	939	14	884	129	451	886	93	347
6	329	1285	595	265	656	249	424	594	28	820	488
7	140	866	1098	19	742	107	668	24	744	105	406
8	54	484	1136	448	181	669	45	629	112	456	453
9	20	236	862	904	25	573	243	371	258	445	98
10	7	103	532	1002	402	102	647	2	591	9	599
11	2	41	282	808	796	44	420	368	134	469	93
12	1	15	133	529	897	394	45	585	67	404	174
13	0	5	57	297	744	730	72	288	451	16	506
14	0	2	23	148	505	813	402	12	494	174	201
15	0	1	8	67	295	682	683	106	181	479	7
16	0	0	3	28	154	473	744	412	0	392	275
17	0	0	1	11	73	285	625	645	141	103	461
18	0	0	0	4	32	153	440	684	420	5	294
19	0	0	0	1	13	76	271	573	610	172	51
20	0	0	0	0	5	35	150	408	631	422	19

ing our value of $D_e''(X)$. We will discuss the form of the barrier and the long range interaction in more detail in a forthcoming paper.[21] Let us just say that from a least-squares fit of the outer turning points (slightly depending on the order of the fit) we obtain a value of the height of the hump of 295 ± 17 cm^{-1} above the $^2P_{3/2} + {}^2S_{1/2}$ atomic levels at an internuclear distance of 8.1 ± 0.1 Å.

In Table V we have summarized the theoretical and experimental values of the most important molecular constants including D_e and R_e, the equilibrium internuclear distance, which so far have been obtained in the literature. The values found by Loomis and Nusbaum[7] and Tango *et al.*[9] are in fair agreement with our much more accurate value. Theoretical calculations of D_e by Müller and Meyer[26] and Ingel-Mann *et al.*[27] have led to the slightly smaller values of 0.537 and 0.53 eV, respectively.

Next, let us discuss the other molecular constants shown in Table V. The agreement of our constants with those of the early work of Loomis and Nusbaum[7] and Loomis[8] is well within the accuracy with which they were able to measure the transitions. However, comparison with the more recent results[11,12] exhibits significant deviations in the rotational constants. The difference with regard to the data of Luh *et al.*[11] is not to be wondered at, as their quoted accuracy is 0.016 cm^{-1}. The disagreement of our Y_{01} and Y_{02} values for the X state with those of Ross *et al.*[12] is outside both quoted accuracies and appears to reflect the difference in the data base used for the computer fit. In particular, the measurements of Ross *et al.* are heavily weighted to larger values of angular momentum and vibrational levels (see their Table I), whereas our basis as shown in Fig. 3 is spread more equally over all values of J. The correctness of the value of Y_{01} plays an important role in the calculation of the potential curve. The abovementioned difference in the rotational constants is reflected in the RKR calculations. Comparison of our potential curve with those of Ross *et al.* indicates a

TABLE V. Comparison of molecular constants of $^{39}K_2$ obtained by various workers. All values are given in cm^{-1}. The figures in parentheses give the error of one standard deviation. $B\,{}^1\Pi_u$ excited state of $^{39}K_2$; $X\,{}^1\Sigma_g^+$ ground state of $^{39}K_2$.

$B\,{}^1\Pi_u$ Ref.	Y'_{10}	Y'_{11}	Y'_{01} (R_e in Å)	Y'_{11} ($\times 10^3$)	Y'_{02} ($\times 10^7$)	D_e	T_e
a	74.73	−0.327	...	...	...	4235	15 377.73
b	(74.73)[a]	(−0.327)[a]	0.048 24 (4.235)	−0.235	−0.806	...	...
l	75.00	−0.3876	...	...	...	1782	15 378.01
m	74.93(34)	−0.378(35)	0.048 692(88) (4.2156)	(−0.24)[b]	−0.765(60)	...	15 375.58
f	74.8817(4)	−0.3269(8)	0.048 220(3) (4.2361)	−0.2309(17)	−0.7960(22)	...	15 377.156
h	74.8911(7)	−0.3274(5)	0.048 225 8(4) (4.235 99)	−0231 04(9)	−0.7994(5)	2113(15)	15 377.1553
$X\,{}^1\Sigma_g^+$ Ref.	Y''_{10}	Y''_{20}	Y''_{01} (R_e in Å)	Y''_{11} ($\times 10^3$)	Y''_{02} ($\times 10^7$)	D_e cm^{-1}	eV
Experiment							
a	92.64	−0.353	...	...	...		
b	(92.64)[a]	(−0.353)[a]	0.056 22 (3.923)	−0.219	−0.828	4146	0.51
c	92.021	0.282 9	0.056 743 (3.9051)	−0.165	−0.863	4516	0.56
d	92.3633	−0.326 37	0.056 212 (3.9235)	−0.212 21	−0.8743		
e	92.4054(4)	−0.327 6(1)	0.056 161(1)	−0.211 9(1)	−0.7986(6)		
f	92.3994(11)	−0.328 0(4)	0.056 18(3) (3.9246)	−0.212 3(4)	−0.8300(25)		
g	...	...	...	...	...	4441(5)	0.5506(6)
h	92.3985(1)	−0.325 72(3)	0.056 186 9(6) (3.924 33)	−0.211 06(2)	−0.8316(5)	4447(15)	0.551(2)
Theory							
i	87	...	0.057 (3.90)	...	...	3950	0.49
j	91.8	−0.26	0.056 (3.93)	−0.24	...	4330	0.537
k	92	...	0.057 (3.90)	...	...	4270	0.53

[a] Reference 35. [b] Reference 8. [c] Reference 9. [d] Reference 11. [e] Reference 12. [f] Reference 1. [g] Reference 36. [h] This work. [i] Reference 37. [j] Reference 27. [k] Reference 28. [l] Reference 7. [m] Reference 10.

uniform shift of 0.001 Å toward smaller values of the internuclear separation. The values of the vibrational energies agree throughout the entire potential curve within the quoted accuracy of each portion of the spectrum.

As a test of the consistency of the constants, we calculate the value of D_e based on the well-known relation first given by Kratzer,[28]

$$D_e = -Y_{02} = 4(Y_{01})^3/(Y_{10})^2.$$

The calculated value of Y_{02} for the B state from the results in Table I is $7.997\,79\times10^{-8}$ cm^{-1}, which deviates from the fit value by 0.075%. For the ground state this calculation gives $Y_{02} = 8.3107\times10^{-8}$ cm^{-1}, a deviation of 0.048% from the fit value. In both cases the deviation lies within the standard deviation of the calculation of the constants. The Y_{02} value calculated with the data given in Ref. 12 deviates from the "Kratzer relation" by 3.9%; this discrepancy is large.

By calculating Y_{03} from the relation given by Kemble *et al.*[29]

$$Y_{03} = 2Y_{02}[12(Y_{01})^2 - Y_{11}Y_{10}]/3(Y_{10})^2,$$

we also find satisfactory agreement with our fit values for both the ground state and the B state.

We investigate the centrifugal distortion terms D_v, H_v, and L_v more carefully to find out to what extent unique relationships between these higher order centrifugal distortion coefficients and the G_v and B_v terms are obeyed. In 1973, Albritton *et al.*[30] gave explicit expressions for these coefficients from a quantum mechanical perturbation approach based on a "rotating vibrator" model. We apply a method described by Hutson[31,32] for calculating the D_v, H_v, and L_v terms using the B- and X-molecular potentials of Tables II and III. His method gives reliable D_v, H_v, ... for all v of the data base while the perturbation approach[30] requires explicit information on continuum levels for calculations at high v. In addition, it works much faster for practical applications. The calculated values are compared with the corresponding values using the constants obtained from Table I. The results show excellent agreement, i.e., for the lower $X\,^1\Sigma_g^+$ state and $v''\leqslant26$ the difference $\Delta D_v''$ is smaller than the standard error. The same is true for the upper $B\,^1\Pi_u$ state and $v'\leqslant40$. The H_v values differ no more than the corresponding standard errors for the lower $X\,^1\Sigma_g^+$ state and $v''\leqslant15$ and for the upper $B\,^1\Pi_u$ state and $v'\leqslant20$. It is well known that the physical significance of fitted Dunham parameters decreases going from D_v to H_v to L_v, etc.; nevertheless, the L_v terms determined at low vibrational quantum numbers which are the highest order centrifugal distortion terms of statistical significance in Table I, differ from the corresponding calculated values by 14% for the ground state and 10% for the excited B state.

The Λ-type doubling in the $B\,^1\Pi_u$ state depends on this state as well as on the $A\,^1\Sigma_u^+$ state which is the only perturbing state to be considered, since it is the only state belonging to the same complex,[33] i.e., $l=1$ for the separated atoms. Our value y_{01} of the Λ-doubling constant agrees very well with the result of the calculation based on van Vleck's model of "pure precession"[34] which gives $y_{01} = 2.52\times10^{-6}$ cm^{-1}.

The correction to the B_v coefficient due to the vibration as given by y_{11}, however, which is expected to be $y_{11} = 2y_{01}Y_{11}/Y_{01} = 2.5\times10^{-8}$ cm^{-1} differs considerably from the fit value. The ratio y_{11}/y_{01} equals $-2\alpha_e/B_e = 2Y_{11}/Y_{01}$, where B_e and α_e represent the "effective" rotational constant for the two states, i.e., these quantities are not precisely defined in terms of the molecular parameters of either state. Loomis[8] determined the Λ-doubling coefficient, which agrees with our much more accurate value within his experiment error.

V. CONCLUSIONS

The combination of polarization spectroscopy with optical interferometric measuring techniques has made possible the measurement of parts of the K_2 $B\,^1\Pi_u$–$X\,^1\Sigma_g^+$ molecular band system with a precision of two parts in 10^8. Furthermore, through calibration of the interferometer via comparison with absolute secondary standards, this precision refers to the absolute accuracy with which these wavelengths can be determined. It has become possible, via this scheme, to reproduce the absolute frequencies to the same accuracy as the relative frequency. However, limitations of this technique caused by inadequately populated quantum levels prohibit the extension of the measurements at this level throughout the entire sytem. Consequently, a description of the system via molecular constants is restricted to the precision of the transitions less well measured. Nevertheless, we have been able to extend the polarization spectroscopy analysis to include 30% of the ground state and nearly all of the B-state levels in the polynomial analysis. The constants obtained in this fashion provide a description of the K_2 $B\,^1\Pi_u$–$X\,^1\Sigma_g^+$ band system to an overall accuracy of five parts in 10^8 for these regions, i.e., total standard deviation of 0.0007 cm^{-1}. This implies that this K_2 system now belongs to those molecular dimers which are spectroscopically the best known. The dissociation energies and the potential barrier of the excited $B\,^1\Pi_u$ state have been determined. Franck–Condon factors have been calculated over the range of vibrational levels measured with very high resolution. There are, however, some residual problems. The rovibrational energies of levels in the X ground state with relatively high v'' and J'' are not, in the present analysis, as accurately described as the energies of states with lower v'' and J''. It would be useful to extend the range of both v'' and J''. Alternatively, new laser spectroscopic techniques may yield data in presently unexplored regions of the ground state.

ACKNOWLEDGMENTS

We wish to thank Thomas Huth and Jörg Nunnenkamp for their help in the earlier stage of the experiment. We would like also to thank the Deutsche Forschungsgemeinschaft, SFB 216 "Polarisation und Korrelation in atomaren Stosskomplexen" and the National Science Foundation, under Grant No. INT-8303911, whose support made this collaborative venture possible. We thank Professor Dieter Beck for helpful discussions and the use of part of his laboratory facilities. Finally, we thank Dr. Jeremy M. Hutson and Professor Richard N. Zare for supplying us with computer programs.

[1]F. Engelke, H. Hage, and U. Schühle, Chem. Phys. Lett. **106**, 535 (1984).
[2]C. D. Caldwell, J. JiMenez-Mier, P. Zhao, F. Engelke, H. Hage, and U. Schühle, J. Opt. Soc. Am. **B2**, 411 (1985), where absolute wavelengths are converted into frequencies adopting the definition of the meter.
[3]M. Raab, G. Hönig, R. Castell, and W. Demtröder, Chem. Phys. Lett. **66**, 307 (1979).
[4]J. L. Hall, Science **202**, 147 (1978).
[5]C. Wieman and T. W. Hänsch, Phys. Rev. Lett. **36**, 1170 (1976).
[6]S. R. Amin, J. Opt. Soc. Am. **73**, 862 (1983).
[7]F. W. Loomis and R. E. Nusbaum, Phys. Rev. **39**, 89 (1932).
[8]F. W. Loomis, Phys. Rev. **38**, 2153 (1931).
[9]W. J. Tango, J. K. Link, and R. N. Zare, J. Chem. Phys. **49**, 4264 (1968).
[10]M. Allegrini, P. Bicci, M. Civilini, and L. Moi, Chem. Phys. Lett. **91**, 63 (1982).
[11]W.-T. Luh, V. Zafiropulos, P. D. Kleiber, W. C. Stwalley, and S. P. Henegan, J. Mol. Spectrosc. **111**, 327 (1985).
[12]A. J. Ross, P. Crozet, J. d'Incan, and C. Effantin, J. Phys. B **19**, L145 (1986).
[13]W. Lichten, J. Opt. Soc. Am. A **2**, 1869 (1985).
[14]W. Lichten, J. Opt. Soc. Am. A **3**, 909 (1986).
[15]T. R. Wik, W. Bennett, Jr., and W. Lichten, Phys. Rev. Lett. **40**, 1080 (1978).
[16]T. Huth, Diplomarbeit, University of Bielefeld, 1985 (unpublished).
[17]See AIP document No. PAPS JCPSA-87-45-32 for 32 pages of the line positions of the K_2 B–X band system. Order by PAPS number and journal reference from American Institute of Physics, Physics Auxiliary Publication Service, 335 East 45th Street, New York, NY 10017. The price is $1.50 for each micofiche (98 pages) or $5.00 for photocopies of up to 30 pages, and $0.15 for each additional page over 30 pages. Airmail additional. Make checks payable to the American Institute of Physics.
[18]D. L. Albritton, A. L. Schmeltekopf, and R. N. Zare, *Molecular Spectroscopy: Modern Research*, edited by K. N. Rao (Academic, New York, 1976), Vol. 2.
[19]J. L. Dunham, Phys. Rev. **41**, 721 (1932).
[20]R. N. Zare, J. Chem. Phys. **40**, 1934 (1964).
[21]J. Heinze and F. Engelke, Z. Phys. D (submitted).
[22]J. Heinze, Dissertation, University of Bielefeld, 1987.
[23]M. S. Child, J. Mol. Spectrosc. **53**, 280 (1974).
[24]R. J. LeRoy and R. B. Bernstein, J. Chem. Phys. **52**, 3869 (1970).
[25]W. Müller, J. Flesch, and W. Meyer, J. Chem. Phys. **80**, 3297 (1984).
[26]W. Müller, and W. Meyer, J. Chem. Phys. **80**, 3311 (1984).
[27]G. Ingel-Mann, U. Wedig, P. Fuentealba, and H. Stoll, J. Chem. Phys. **84**, 5007 (1986).
[28]A. Kratzer, Z. Phys. **3**, 289 (1920).
[29]E. C. Kemble, R. T. Birge, W. F. Colby, F. W. Loomis, and L. Page, *Molecular Spectra in Gases* (National Research Council, Washington, D.C., 1930), p. 57.
[30]D. L. Albritton, W. J. Harrop, A. L. Schmeltekopf, and R. N. Zare, J. Mol. Spectrosc. **46**, 25 (1973).
[31]J. M. Hutson, J. Phys. B **14**, 851 (1981).
[32]J. M. Hutson and B. Howard, Mol. Phys. **41**, 1113 (1980).
[33]J. T. Hougen, Natl. Bur. Stand. U.S. Monogr. 115 (1970).
[34]J. H. van Vleck, Phys. Rev. **33**, 467 (1929).
[35]W. O. Crane and A. Christy, Phys. Rev. **36**, 421 (1936).
[36]A. J. Ross, C. Effantin, J. d'Incan, R. F. Barrow, and J. Vergès, Indian J. Phys. B **60**, 309 (1986).
[37]G. H. Jueng, J. P. Daudey, and J. P. Malrieu, J. Phys. B **16**, 699 (1983).